Characterization of phases development in isochronally annealed Mg-Tb-Nd alloy

B. Smola*, I. Stulíková, J. Čížek, J. Černá, M. Vlach

Charles University, Faculty of Mathematics and Physics, Ke Karlovu 5, CZ-121 16 Prague 2, Czech Republic

Received 8 June 2008, received in revised form 16 September 2008, accepted 19 September 2008

Abstract

Three transient and one stable phase precipitate sequentially during isochronal annealing 30 K/30 min and 20 K/20 min in solution heat-treated Mg4Tb2Nd and Mg3Tb2Nd alloys (nominal composition in wt.%). The precipitation of the transient phases is characterized by measurable heat release. Quenched-in vacancies bond to Tb and/or Nd atoms up to 120 °C probably contribute to relatively well-developed early precipitation stages. The dense triangular arrangement of the coherent $D0_{19}$ phase plates is responsible for the peak age hardening observed after annealing up to ∼ 220–270 °C. The peak hardening temperature depends on solute concentration and on solution heat treatment conditions. Following loss of particle coherency during a sequent precipitation of β_1 (fcc structure, lattice parameter $a = 0.74$ nm) and β (fcc structure, Mg_5Gd-type) phases leads to developing of open volume defects at matrix-precipitate interfaces.

K e y w o r d s: Mg alloys, electrical resistivity, DSC, TEM, positron annihilation spectroscopy

1. Introduction

Alloying magnesium with rare earth (R. E.) elements (inclusive Sc and Y) led to the development of successful commercial WE alloy containing Y and Nd [1–3] and promising high performance alloys containing Sc, Mn in combination with Gd, Y, and Y + Nd [4–7]. Mostly relative thermally stable precipitates of transient phases are responsible for peak hardening in Mg-R.E. base alloys.

According to the type of R. E. there are two principal decomposition sequences of supersaturated solid solution [1, 8]:

Mg-Gd (Y) type:
α (cph) → β'' ($D0_{19}$) → β' (cbco) → β (fcc, bcc),
Mg-Ce type:
α (cph) → β'' ($D0_{19}$) → β' (fcc $D0_3$) → β (bct).

When the rare earths of both groups are combined in magnesium alloys a combination of these basic decomposition sequences is observed, e.g. WE 43 alloy (Mg-Y-Nd):
α (cph) → β'' ($D0_{19}$) → β' (cbco) → β_1 (fcc $D0_3$) → β (fcc) [1, 9, 10].

Neither bcc phase of Mg-Y binary alloy, nor bct phase of Mg-Nd system is the equilibrium phase here, instead fcc phase of Mg-Gd binary alloys develops.

For the development of light Mg alloys suited to comply with requirements of different applications in transport, leisure and sport industry and in other possible applications such as biomaterials the complex characterization of the properties of phases is highly desirable. Simultaneous application of different physical methods such as electrical resistometry, differential scanning calorimetry (DSC) and positron annihilation spectroscopy (PAS) together with microstructure study by transmission electron microscopy is used as one of such a complex characterization (e.g. for commercial alloy WE43 [11]). As similar decomposition sequences and transient and equilibrium phases occur in Mg alloys with R. E. elements it is worthwhile to carry out complex characterization also of model Mg alloys with the combination of R. E.

In this paper the results of resistivity changes, mi-

*Corresponding author: tel.: +420 221 911 355; fax: +420 221 911 618; e-mail address: smola@met.mff.cuni.cz

Table 1. Composition of Mg4Tb2Nd and Mg3Tb2Nd alloys

Notation	Tb (wt.%)	Nd (wt.%)	Solution heat treatment
Mg4Tb2Nd	3.96	2.53	500 °C/4 h
Mg3Tb2Nd	3.15	1.75	525 °C/6 h

crostructure and positron life-time (PL) response to the isochronal annealing of MgTbNd alloys are compared with DSC results.

2. Experimental details

The Mg4Tb2Nd and Mg3Tb2Nd alloys were squeeze cast under a protective gas atmosphere (Ar + 1%SF6). Their actual composition is listed in Table 1. The Mg4Tb2Nd alloy was solution treated at 500 °C for 4 h, the Mg3Tb2Nd one at 525 °C for 6 h. The grain size increased to about 400 μm and did not change during following isochronal heat treatment.

The response of the relative electrical resistivity changes to isochronal annealing was measured over the range 20–480 °C. Annealing of the Mg4Tb2Nd alloy was carried out in steps of 30 K/30 min. Each annealing step was followed by quenching. Heat treatment was performed in a stirred oil bath up to 240 °C or in a furnace with an argon protective atmosphere at higher temperatures. Relative electrical resistivity changes ρ/ρ_0 were obtained with an accuracy of 10^{-4}. The resistivity was measured at temperature of liquid N_2 using the dc four-point method with a dummy specimen in series. The influence of parasitic thermo-electromotive forces was suppressed by current reversal.

The thermal stability of the mechanical properties during isochronal heat treatment was monitored by Vickers hardness HV 3 at room temperature. Transmission electron microscopy (TEM) and electron diffraction were carried out to determine the microstructure of the alloy after specified treatments. An analysis of the phases precipitated was also supported by energy-dispersive X-ray microanalysis. Studies of the microstructure were undertaken on a JEOL JEM 2000FX and a Philips 200CM electron microscopes equipped with a LINK AN 1000 and an EDAX microanalyser, respectively. The specimens for TEM were prepared by the same isochronal annealing procedure as those for electrical resistivity and hardness measurements.

The same isochronal annealing procedure (but in the steps 20 °C/20 min) was applied to specimens of the Mg3Tb2Nd alloy for positron life-time spectroscopy. The fast-fast PL spectrometer with time resolution of 160 ps was used. Detailed description of the spectrometer can be found in [12]. The development of Vickers microhardness HV 0.01 was measured during the same 20 °C/20 min isochronal heat treatment.

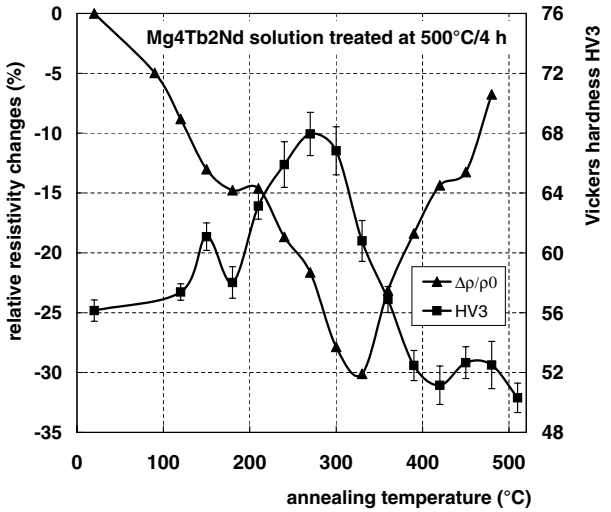

Fig. 1. Resistivity at 77 K and hardness response on isochronal annealing of Mg4Tb2Nd alloy solution treated at 500 °C/4 hours.

Differential scanning calorimetry of the Mg4Tb2Nd alloy was performed at heating rates 5 and 10 K min^{-1} on Netzch DSC 200 F3 apparatus. Specimens of the alloy were heated on air in Al_2O_3 crucibles up to 500 °C with pure Mg as comparison specimen.

3. Results and discussion

The resistivity response and the response of Vickers hardness to isochronal annealing of the solution treated Mg4Tb2Nd alloy are shown in Fig. 1. The resistivity drops to about 70 % of its initial value by annealing up to temperature 330 °C in three stages. The first one is completed at ∼ 180 °C and is connected with a small local hardness maximum. The peak hardening was observed in the second decrease stage in the annealing temperature range ∼ 210–250 °C. The hardness diminishes in the third resistivity decrease stage at ∼ 250–330 °C. The following steep resistivity increase is detained in the annealing temperature range ∼ 420–450 °C, where also slight hardness increase was observed.

A resistivity decrease and simultaneous hardness increase are typical for precipitation processes. This is supported by DSC measurements performed on the same alloy after the same solution treatment. Three observed reactions with maxima of heat flow at 175 °C, 285 °C and 377 °C for heating rate of 10 K min^{-1}

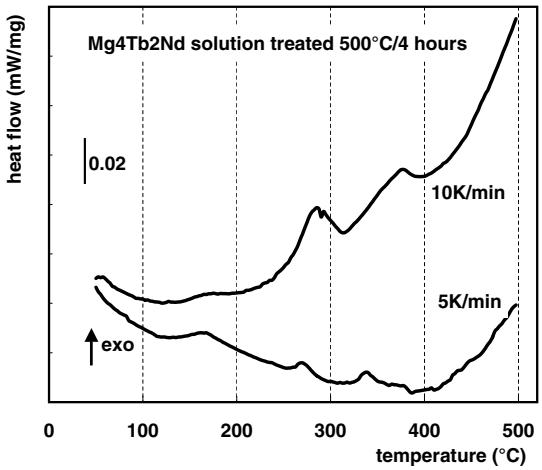

Fig. 2. DSC curves of Mg4Tb2Nd alloy solution treated at 500 °C/4 hours at heating rates 5 K min^{-1} and 10 K min^{-1}.

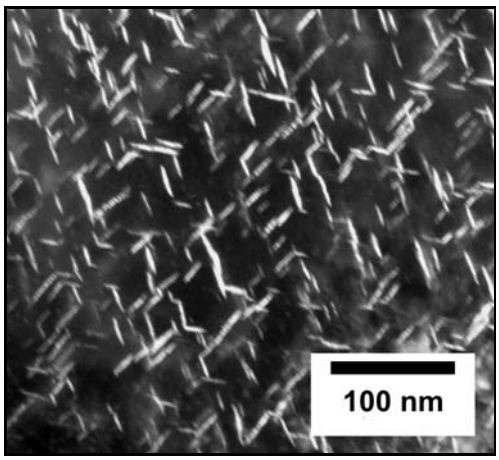

Fig. 3. Triangular arrangement of $D0_{19}$ phase prismatic plates parallel to $\{11\bar{2}0\}_{Mg}$ planes in Mg4Tb2Nd alloy annealed up to 270 °C.

are exothermic and shifted to lower temperature for 5 K min^{-1} heating rate – Fig. 2.

The detailed microstructure observation showed that four precipitation processes took place in a sequence during isochronal annealing [8, 13]. After annealing up to 180 °C diffused diffraction spots of the $D0_{19}$ phase appear, which indicates fine spherical particles of this coherent phase. By annealing up to 240 °C the $D0_{19}$ phase develops to the plates parallel to all equivalent $\{11\bar{2}0\}_{Mg}$ planes (diameter ∼ 15–30 nm, thickness ∼ 1 nm). This morphology of the $D0_{19}$ phase prevails during annealing up to 270 °C (Fig. 3) where very weak diffraction spots of the cbco phase were detected. The low diffraction intensity suggest only very low volume fraction of this phase. The dense triangular arrangement of the $D0_{19}$ phase plates is responsible

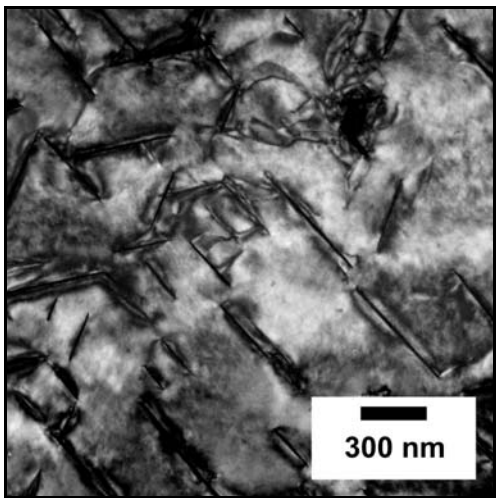

Fig. 4. Triangular arrangement of β_1 prismatic plates parallel to $\{10\bar{1}0\}_{Mg}$ planes in Mg4Tb2Nd alloy annealed up to 330 °C.

for the peak age hardening observed after annealing up to 270 °C – see Fig. 1.

Further annealing up to 330 °C leads to the transformation of the $D0_{19}$ phase into β_1 phase and its further precipitation in the form of plates parallel to all equivalent $\{10\bar{1}0\}_{Mg}$ planes (fcc structure, diameter ∼ 600 nm, thickness ∼ 20 nm) – Fig. 4. This process leads to the further resistivity decrease due to the solute concentration decrease in the α-Mg matrix. The hardness decreases markedly as the size, aspect ratio and number density of the β_1 phase plates are significantly lower than those of the $D0_{19}$ phase (cf. Figs. 3 and 4). The plates of the stable phase (fcc structure, Mg_5Gd-type) develop after annealing up to 390 °C. They are parallel to the same planes as those of β_1 phase. The diameter is about 0.5–1 μm and thickness is ∼ 30 nm. The β plates were observed even after an isochronal anneal up to 450 °C with increased thickness (∼ 50 nm) but with negligible increase in diameter.

Solution treated Mg3Tb2Nd alloy exhibits a two component positron life-time spectrum consisting of $\tau_1 = (220 \pm 1)$ ps with the relative intensity of $I_1 = (91 \pm 1)$ % and $\tau_2 = (280 \pm 20)$ ps with the intensity of $I_2 = (9 \pm 1)$ %. The major component belongs to free delocalized positrons, the minor one comes from positrons trapped at quenched-in vacancies bound to Tb or Nd atoms [14]. The existence of vacancy-solute atom complexes can contribute to relatively early precipitation of the β'' phase spheres and consequently to the existence of well developed plates of this phase during following annealing. No contribution of positrons trapped at dislocations was observed. The τ_2 component disappears after the isochronal annealing up to 120 °C and is replaced above 280 °C by a component of the life-time $\tau_3 = 256$ ps

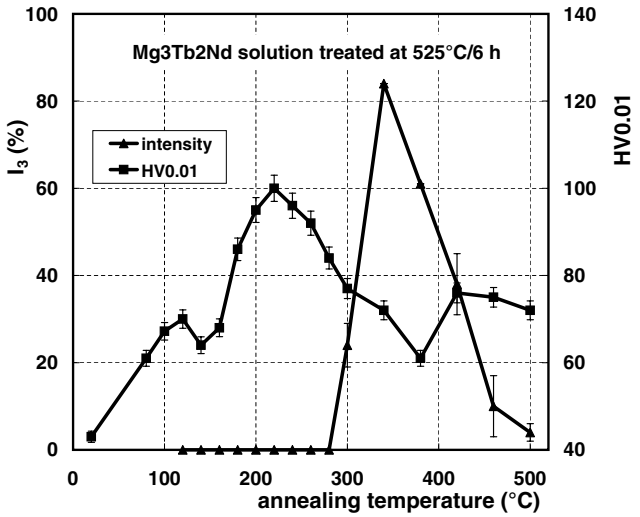

Fig. 5. Intensity development of positrons trapped at precipitate interfaces and microhardness development with isochronal annealing (20 K/20 min) of Mg3Tb2Nd alloy solution treated at 525 °C/6 hours.

of varying intensity I_3. Its development with annealing temperature is shown in Fig. 5 together with that of microhardness HV 0.01 measured by the same isochronal annealing procedure in the solution treated Mg3Tb2Nd alloy.

Only one component spectrum was observed in the temperature range 120–280 °C, which means that the microstructure development does not lead to active positron traps. It is in accordance with the fact that β'' particles are fully coherent with the Mg lattice and, therefore, no open volume defects are introduced by this phase precipitation. As soon as the transformation of β'' to β_1 phase plates starts, a defect component τ_3 appears with intensity reaching the maximum after the annealing up to 340 °C. Positrons are, most probably, trapped at misfit defects in the precipitate – matrix interfaces. The β_1 phase has fcc structure with lattice parameter $a = 0.74$ nm and is incoherent to the Mg matrix. The intensity I_3 decreases when the β_1 precipitates dissolve. This decrease is retarded in the annealing temperature range 390–450 °C, where the development of stable β phase (plate shaped particles of 2–3 μm in diameter, fcc structure isomorphic with Mg_5Gd, $a = 2.23$ nm) was detected. Fraction of positrons trapped at β phase particles is lower than that in β_1 phase precipitates most probably due to much smaller interface area of β phase particles compared to that of β_1 phase plates.

The response of microhardness corresponds well to the microstructure development. The most pronounced hardening is caused by the β'' plates in a triangular arrangement, if they have an optimal size (after isochronal annealing up to 220 °C), but all four various types of precipitates contribute positively to microhardness. Local peaks of the isochronal annealing microhardness HV 0.01 curve are shifted to lower temperatures comparing it to the isochronal annealing curve of hardness HV 3 measured for the alloy with a little higher content of Tb and Nd in Mg and the same effective annealing rate (1 K/1 min) – compare the HV 3 and HV 0.01 annealing curves in Fig. 5 and Fig. 1. The absolute values of HV 0.01 are higher than those of HV 3 and the relative hardening achieved is higher for the Mg3Tb2Nd alloy (132 % for the Mg3Tb2Nd and only 21 % for the Mg4Tb2Nd). Despite the fact that these quantities can be influenced by grain boundary properties in slightly different way, the comparison indicates that the higher temperature and time of solution treatment lead to significantly higher supersaturation of solid solution even if the concentration of Tb and Nd additives was lower.

4. Conclusions

1. Three transient and one stable phase precipitate sequentially during the isochronal annealing with the constant effective heating rate of 1 K min^{-1} in studied MgTbNd alloys. Precipitation of transient phases exhibits exothermal reactions.

2. In the Mg4Tb2Nd alloy the β'' phase ($D0_{19}$ structure, fully coherent to the Mg matrix) precipitates first as spheres and transforms to plates in a triangular arrangement at 210–270 °C. This phase develops to the β_1 phase above 270 °C, it has the fcc structure ($a = 0.74$ nm) and is incoherent to the matrix. It dissolves above 330 °C. The equilibrium phase β (isomorphic to Mg_5Gd phase, fcc structure, $a = 2.23$ nm) starts to develop above 390 °C. Similar phase development occurs in the Mg3Tb2Nd alloy but at significantly lower temperatures due to the higher solute supersaturation caused by longer solution heat treatment at higher temperature.

3. The peak hardening is connected with the β'' phase plate-like particles arranged in triangles.

4. Quenched-in vacancies are bond to Tb and/or Nd atoms in the temperature range room temperature – 120 °C, that probably contributes to precipitation of the β'' phase at relatively low temperatures.

5. Open volume defects at interfaces between matrix and precipitate particle of the β_1 phase were detected by positron life time spectroscopy. The trapping of positrons was observed also in the range of the equilibrium phase β precipitation, but its intensity is lower due to much smaller interface area (particle size 2–3 μm).

Acknowledgements

We would like to dedicate this article to Prof. Michal Boček on the occasion of his 80th birthday. The financial

support by Czech Science Foundation within the framework of the project Nr. 106/06/0252 is gratefully acknowledged.

References

[1] LORIMER, G. W.: In: Proc. London Conf. Magnesium Technology. Ed.: Baker, H. London, Inst. of Metals 1986, p. 47.
[2] POLMEAR, I. J.: Mater. Sci. Technol., *10*, 1994, p. 1.
[3] VOSTRÝ, P.—STULÍKOVÁ, I.—SMOLA, B.—CIESLAR, M.—MORDIKE, B. L.: Z. Metallkde, *79*, 1988, p. 340.
[4] SMOLA, B.—STULÍKOVÁ, I.—von BUCH, F.—MORDIKE, B. L.: Mat. Sci. Eng. A, *324*, 2002, p. 113.
[5] STULÍKOVÁ, I.—SMOLA, B.—von BUCH, F.—MORDIKE, B. L.: Mat.-wiss. u. Werkstofftech., *34*, 2003, p. 102.
[6] NEUBERT, V.—STULÍKOVÁ, I.—SMOLA, B.—BAKKAR, A.—MORDIKE, B. L.: Kovove Mater., *42*, 2004, p. 31.
[7] MORDIKE, B. L.—STULÍKOVÁ, I.—SMOLA, B.: Metall. Mater. Trans. A, *36*, 2005, p. 1729.
[8] SMOLA, B.—STULÍKOVÁ, I.: Kovove Mater., *42*, 2004, p. 301.
[9] NIE, J. F.—MUDDLE, B. C.: Acta Mater., *48*, 2000, p. 1691.
[10] ANTION, C.—DONNADIEU, P.—PERRARD, F.—DESCHAMPS, A.—TASSIN, C.—PISCH, A.: Acta Mater., *51*, 2003, p. 5335.
[11] MENGUCCI, P.—BARUCCA, G.—RIONTINO, G.—LUSSANA, D.—MASSAZZA, M.—FERRAGUT, R.—HASSAN ALLY, E.: Mater. Sci. Eng. A, *479*, 2008, p. 37.
[12] BEČVÁŘ, F.—ČÍŽEK, J.—LEŠŤÁK, L.—NOVOTNÝ, I.—PROCHÁZKA, I.—ŠEBESTA, F.: Nucl. Instr. Meth. A, *443*, 2000, p. 557.
[13] NEUBERT, V.—STULÍKOVÁ, I.—SMOLA, B.—MORDIKE, B. L.—VLACH, M.—BAKKAR, A.—PELCOVÁ, J.: Mater. Sci. Eng. A, *462*, 2007, p. 329.
[14] ČÍŽEK, J.—PROCHÁZKA, I.—SMOLA, B.—STULÍKOVÁ, I.—VLACH, M.—ISLAMGALIEV, R. K.—KULYASOVA, O.: Mater. Sci. Forum, *584–586*, 2008, p. 591.